AGU PUBLICATIONS

Geophysical Research Letters

RESEARCH LETTER
10.1002/2015GL065702

Key Points:
- The ozone depletion potential of N_2O (ODP-N_2O) is sensitive to CO_2 and CH_4
- ODP-N_2O in 2100 is larger than in 2000 and varies by up to a factor of 2
- A single-valued ODP-N_2O is of limited use

Supporting Information:
- Table S1

Correspondence to:
L. E. Revell,
laura@bodekerscientific.com

Citation:
Revell, L. E., F. Tummon, R. J. Salawitch, A. Stenke, and T. Peter (2015), The changing ozone depletion potential of N_2O in a future climate, *Geophys. Res. Lett.*, *42*, 10,047–10,055, doi:10.1002/2015GL065702.

Received 6 AUG 2015
Accepted 30 SEP 2015
Published online 23 NOV 2015

The changing ozone depletion potential of N_2O in a future climate

L. E. Revell[1,2], F. Tummon[1], R. J. Salawitch[3,4,5], A. Stenke[1], and T. Peter[1]

[1]Institute for Atmospheric and Climate Science, ETH Zurich, Zurich, Switzerland, [2]Bodeker Scientific, Alexandra, New Zealand, [3]Department of Atmospheric and Oceanic Science, University of Maryland, College Park, Maryland, USA, [4]Department of Chemistry and Biochemistry, University of Maryland, College Park, Maryland, USA, [5]Earth System Science Interdisciplinary Center, University of Maryland, College Park, Maryland, USA

Abstract Nitrous oxide (N_2O), which decomposes in the stratosphere to form nitrogen oxides (NO_x), is currently the dominant anthropogenic ozone-depleting substance emitted. Ozone depletion potentials (ODPs) of specific compounds, commonly evaluated for present-day conditions, were developed for long-lived halocarbons and are used by policymakers to inform decision-making around protection of the ozone layer. However, the effect of N_2O on ozone will evolve in the future due to changes in stratospheric dynamics and chemistry induced by rising levels of greenhouse gases. Despite the fact that NO_x-induced ozone loss slows with increasing concentrations of CO_2 and CH_4, we show that ODP_{N2O} for year 2100 varies under different scenarios and is mostly larger than ODP_{N2O} for year 2000. This occurs because the traditional ODP approach is tied to ozone depletion induced by CFC-11, which is also sensitive to CO_2 and CH_4. We therefore suggest that a single ODP for N_2O is of limited use.

1. Introduction

Nitrous oxide (N_2O) is a long-lived greenhouse gas (GHG) with both natural and anthropogenic sources. Since preindustrial times its atmospheric concentration has increased from ~270 ppb to 322 ppb [*Montzka et al.*, 2011], and it is projected to continue increasing through the 21st century [*Meinshausen et al.*, 2011]. N_2O is destroyed mainly in the stratosphere, where it can either be photolyzed or undergo reaction with excited atomic oxygen ($O(^1D)$). This latter process produces nitrogen oxides ($NO_x = NO + NO_2$), which catalyze ozone destruction [*Crutzen*, 1970].

Increases in GHGs alter the chemical, dynamical and radiative environment of the stratosphere such that the effectiveness of N_2O in destroying ozone is weakened, as discussed below. Increased concentrations of GHGs cool the stratosphere, and under cooler conditions the NO_x-induced ozone destruction cycle slows, and second more NO_x is converted to N_2, which is inert and does not react with ozone [*Rosenfield and Douglass*, 1998]. In addition, the meridional stratospheric circulation (the Brewer-Dobson circulation) is projected to strengthen as GHG concentrations increase, which means that N_2O is converted less efficiently into odd nitrogen ($NO_y = NO_x + N + NO_3 + 2 \times N_2O_5 + HNO_3 + HNO_4 + ClONO_2 + BrONO_2$), resulting in reduced abundances of stratospheric NO_y overall because there is less time for the photochemical decay of N_2O when air ascends more rapidly from the troposphere [*Plummer et al.*, 2010].

In addition to these general GHG effects, some effects of specific GHGs on NO_x chemistry are worthy of mention. Increases in stratospheric N_2O mean that more NO_x-induced ozone loss occurs in the middle stratosphere, which allows more UV to penetrate the middle stratosphere and photolytically destroy N_2O; thus N_2O can shorten its own lifetime by 10–15% [*Myhre and Shindell*, 2013; *Prather*, 1998]. Moreover, stratospheric NO_x-induced ozone depletion can also be slowed by increases in CH_4, which produces reactive hydrogen ($HO_x = H + OH + HO_2$). OH may also react with NO_2 to produce HNO_3, thereby converting reactive NO_x to NO_y reservoir species that do not react with ozone:

$$OH + NO_2 + M \rightarrow HNO_3 + M \quad \text{(R1)}$$

An analogous process occurs with stratospheric chlorine ($Cl_y = Cl + 2 \times Cl_2 + ClO + 2 \times Cl_2O_2 + ClONO_2 + HCl + HOCl + BrCl$), whereby ClO converts NO_2 to the reservoir species $ClONO_2$ via reaction (R2):

$$ClO + NO_2 + M \rightarrow ClONO_2 + M \quad \text{(R2)}$$

Because of (R2), the ozone depletion potential of N_2O (ODP_{N2O}) is smaller when stratospheric Cl_y concentrations are large [*Ravishankara et al.*, 2009; *Fleming et al.*, 2011]. However, the concentration of stratospheric Cl_y is projected to be smaller at the end of the 21st century than it was in 1980 due to the Montreal Protocol on Substances that Deplete the Ozone Layer [*World Meteorological Organization (WMO)*, 2011; *Harris and Wuebbles*, 2014], so reaction (R2) will not be a significant process for the 2100 timeframe which we examine.

Based on the effects of GHGs on ozone-depleting NO_x chemistry discussed above, the effectiveness of N_2O in destroying stratospheric ozone is not expected to increase at a commensurate rate with projected increases in surface N_2O concentrations through the 21st century. Indeed, *Revell et al.* [2012a, 2012b] showed that depending on the GHG scenario, stratospheric NO_x-induced ozone loss may decrease through the 21st century despite increasing surface concentrations of N_2O.

Prior studies have quantified the effectiveness of N_2O in depleting stratospheric ozone by calculating an ozone depletion potential for N_2O [*Ravishankara et al.*, 2009; *Fleming et al.*, 2011; *Portmann et al.*, 2012]. Insofar, as we are aware, only one study to date has quantified by how much ODP_{N2O} might change between 2000 and 2100: *Fleming et al.* [2011] used a single scenario applying surface boundary conditions of ozone-depleting substances (ODSs) from the World Meteorological Organization's (WMO) A1 scenario (2007) [*WMO*, 2007] and GHG boundary conditions from scenario A1B (medium) of the Intergovernmental Panel on Climate Change's Special Report on Emissions Scenarios [*Nakicenovic and Swart*, 2000]. Their two-dimensional model calculations suggest that ODP_{N2O} decreases by 5%, from 0.019 to 0.018 between 2000 and 2100. In contrast, we show here that ODP_{N2O} in 2100 may be twice as large than in 2000, depending on the CO_2 and CH_4 concentrations.

Our study differs from previous studies in that we use a range of scenarios based on the recent Representative Concentration Pathways (RCPs) [*Meinshausen et al.*, 2011]. Furthermore, to more accurately capture the coupled chemical and dynamical changes of the stratosphere, we employ here for the first time a three-dimensional chemistry-climate model (CCM) for such a study, rather than a two-dimensional model [*Ravishankara et al.*, 2009; *Daniel et al.*, 2010; *Fleming et al.*, 2011; *Portmann et al.*, 2012; *Stolarski et al.*, 2015]. While ozone-depleting NO_x chemistry (and therefore ODP_{N2O}) is affected by many factors including the concentrations of CO_2, CH_4, N_2O, and Cl_y (as discussed above), we focus here on quantifying the sensitivity of ODP_{N2O} to CO_2 and CH_4 concentrations. These are the two dominant anthropogenic GHGs and provide a clear example of why a single-valued ODP_{N2O} is of limited use.

2. Computational Methods

2.1. The SOCOL Chemistry-climate Model

Simulations were performed with version 3 of the SOCOL (Solar Climate Ozone Links) CCM [*Stenke et al.*, 2013; *Revell et al.*, 2015], which is based on the general circulation model MA-ECHAM5 (middle-atmosphere European Centre Hamburg Model Fifth Generation) [*Roeckner et al.*, 2003]. SOCOL includes 41 chemical species, 140 gas-phase reactions, 46 photolysis reactions, and 16 heterogeneous reactions, plus a further 16 organic species and 44 chemical reactions, which make up the condensed isoprene mechanism Mainz Isoprene Mechanism version 1 [*Poeschl et al.*, 2000]. Chemical species are advected by a flux-form semi-Lagrangian scheme [*Lin and Rood*, 1996]. For the present study, SOCOL was run with 39 vertical levels between the Earth's surface and 0.01 hPa (approximately 80 km), and T42 horizontal resolution, which corresponds approximately to grid cell sizes of $2.8° \times 2.8°$.

2.2. Simulations

To calculate ODP_{N2O}, SOCOL was run in time-slice mode (that is, continuous repeating conditions for a given year) for 5 years before the simulation branched; either with a continuous addition of CFC-11 (100 ppt) or with a continuous addition of N_2O (50 ppb), to obtain the global-mean total column ozone response once a new steady state was reached (see section 2.3). All simulations were initialized with a 10 year spin-up period, which was not included in our analyses.

We performed simulations for years 2000 and 2100 conditions. The former was conducted so that we could compare our model-calculated ODP_{N2O} to results of other studies, which generally focused on the present. The latter set of runs for 2100, described below, allow us to quantify the sensitivity of the ODP of N_2O to future levels of CO_2 and CH_4. Boundary conditions for the year 2000 simulation were based on observations

and used prescribed values for greenhouse gases and ODSs, tropospheric ozone precursor emissions [*Lamarque et al.*, 2010], stratospheric aerosol surface area densities [*Arfeuille et al.*, 2013; *Luo*, 2013], sea surface temperatures, and sea ice concentrations [*Rayner et al.*, 2003].

To explore the range of possible ODP_{N2O} under different future atmospheric conditions, we performed nine sensitivity simulations for the year 2100. All simulations were based on RCP 6.0, a medium-high climate scenario [*Masui et al.*, 2011], but differed in the CH_4 and CO_2 surface concentrations. CO_2 was set to either 370 ppm, 655 ppm, or 940 ppm and CH_4 was set to either 1250 ppb, 2502 ppb, or 3755 ppb. The CO_2 and CH_4 concentrations were selected to cover the full range of concentrations encompassed by RCPs 2.6, 4.5, 6.0, and 8.5 between 2000 and 2100. N_2O concentrations adhered to RCP 6.0 in 2100 for all simulations (406 ppb), as did tropospheric ozone precursor emissions. ODSs followed the WMO's A1 scenario [*WMO*, 2011], which is nearly identical to the scenario for ODSs given by the RCPs. Year 2000 stratospheric aerosol surface area densities [*Luo*, 2013] were used for all simulations, as this was a volcanically quiescent period.

The same (RCP 6.0) year 2100 sea surface temperatures were used for all of the year 2100 sensitivity simulations [*Meehl et al.*, 2013]. This is necessary to isolate the sensitivity of ODP_{N2O} to dynamical and chemical effects of CO_2 and CH_4. We are confident that this approach is justified for our determinations of ODP_{N2O} because global-mean total column ozone corresponding to 2100 surface mixing ratios found using this approach is quite similar to values found using transient runs of our model, as described in section 3.1.

2.3. ODP Calculations

ODP is defined as the change in globally averaged column ozone induced by a compound of interest at steady state per unit mass emission rate, relative to the same quantity for CFC-11 [*Solomon et al.*, 1992]. Noting that CFC-11 and N_2O are prescribed as surface concentrations rather than emission fluxes in SOCOL, we perturbed the model with a continuous addition of 100 ppt of CFC-11 until a new steady state was reached. This induced a decrease in global-mean total column ozone of approximately 0.5–2.5 Dobson units (DU), depending on the CO_2 and CH_4 concentrations. For a 100 ppt addition of CFC-11, the mass-equivalent concentration of N_2O that should be added to the model is 0.31 ppb; however, this is too small an amount to yield an observable difference in ozone. Instead, we added 50 ppb of N_2O, which induces ozone decreases within the same range as CFC-11. These changes in boundary layer mixing ratios are the same as those chosen by *Ravishankara et al.* [2009]. ODPs were then calculated using the steady state formulation shown in equation (1):

$$ODP_{N2O} = \frac{m_{CFC11} \times \Delta\mu_{CFC11} \times \tau_{N2O} \times [\Delta O_3]_{N2O}}{m_{N2O} \times \Delta\mu_{N2O} \times \tau_{CFC11} \times [\Delta O_3]_{CFC11}} \quad (1)$$

which describes the change in total ozone caused by the N_2O perturbation normalized by the N_2O mass flux relative to the same perturbation caused by CFC-11. In detail, m is the molecular mass of the ODS, τ its atmospheric lifetime (as calculated by the model for each simulation), $\Delta\mu$ a prescribed change in its boundary layer mixing ratio (100 ppt of CFC-11 and 50 ppb of N_2O), and ΔO_3 the resulting change in global-mean total column ozone.

3. Results and Discussion

3.1. Total Column Ozone Projections in 2100

We first examine how global-mean total column ozone responds to the various CO_2 and CH_4 concentrations in the nine sensitivity simulations (Figure 1a). Based on year 2100 annual-mean CO_2 and CH_4 surface mixing ratios defined for the RCPs [*Meinshausen et al.*, 2011], we estimate that global-mean total column ozone in the year 2100 will be 307, 311, 315, and 330 DU for RCP 2.6, 4.5, 6.0, and 8.5, respectively (black squares in Figure 1a). The four future estimates of column ozone for 2100 found using the time slice approach are in close agreement with the 2090s global-mean total ozone columns 307, 312, 311, and 329 DU calculated from transient SOCOL simulations that followed the time evolution of GHGs according to each RCP scenario [*Swiss Federal Institute of Technology Zurich and the Physical-Meteorology Observatory Davos*, 2015]. The transient simulations ran from 2000–2100 and used prescribed boundary conditions for GHGs, tropospheric ozone precursor emissions, sea surface temperatures, and sea ice concentrations following either RCP 2.6, RCP 4.5, RCP 6.0, or RCP 8.5, while ODSs followed the WMO A1 scenario in all four simulations.

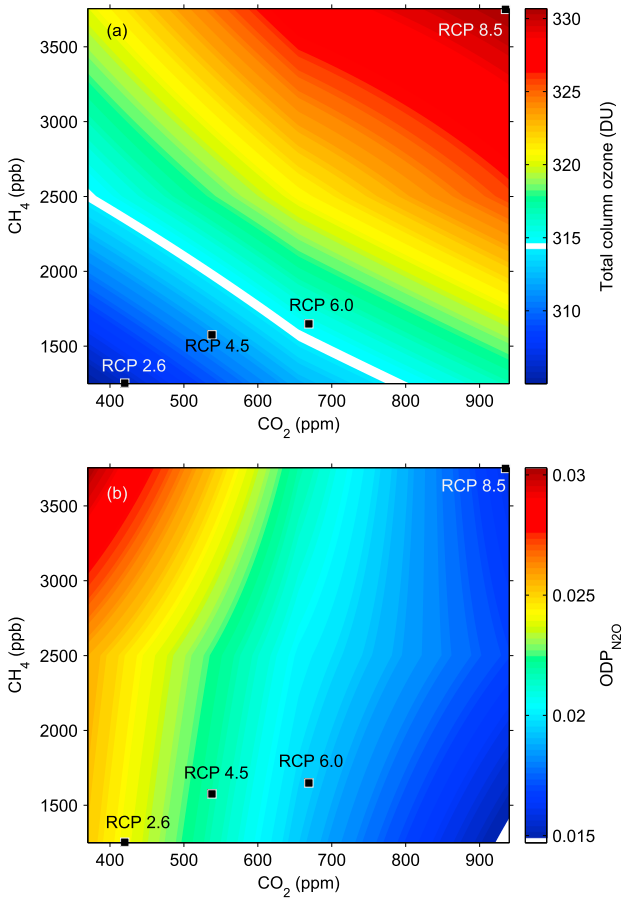

Figure 1. (a) Global-mean total column ozone in 2100 and (b) ODP_{N2O} in 2100 for the nine sensitivity simulations (at corner and center points of each axis), with linear interpolation in between. In both panels, the black squares show values corresponding to the appropriate CO_2 and CH_4 surface concentrations for the RCPs in 2100. The white contour lines show the values of total column ozone (314 DU) and ODP_{N2O} (0.015; bottom right-hand corner) found for year 2000, to give an indication of how these quantities could potentially evolve between 2000–2100 owing to changes in atmospheric composition and circulation.

While it is generally accepted that global stratospheric ozone will increase through the 21st century due to GHG-induced stratospheric cooling and decreasing chlorine loading following the Montreal Protocol, the SOCOL CCM projects that global-mean total column ozone may be larger or smaller in 2100 than in 2000, depending on the greenhouse gas scenario (Figure 1a). The white contour of Figure 1a denotes the value of total column ozone for the year 2000 (314 DU). Although stratospheric column ozone does indeed increase between 2000 and 2100 in our nine sensitivity simulations as well as in all four transient RCP simulations (not shown), tropospheric column ozone decreases in all RCPs except RCP 8.5, following decreases in ozone precursor emissions in RCPs 2.6, 4.5, and 6.0 (also shown previously by *Young et al.* [2013]). Because we prescribed ozone precursor emissions (NO_x, carbon monoxide, and nonmethane volatile organic compounds) corresponding to RCP 6.0 in our nine sensitivity simulations, global-mean tropospheric ozone decreases between 2000 and 2100 in all simulations except for the three with the largest CH_4 surface concentrations (CH_4 itself being an important tropospheric ozone precursor). The declines in global-mean total column ozone in 2100 shown in Figure 1a correspond to situations where the calculated decreases in tropospheric column ozone exceed the computed rise in stratospheric ozone. However, SOCOL systematically overestimates global-mean tropospheric ozone [*Revell et al.*, 2015], and other models do not simulate reductions in total column ozone between 2000 and 2100 following the RCPs [*Eyring et al.*, 2013; *Pawson and Steinbrecht*, 2014]. *Eyring et al.* [2013] have suggested that total column ozone should not be used as a proxy for stratospheric column ozone, given that the large influence tropospheric ozone will have on future total column ozone. However, we shall examine changes in total column ozone, since our focus is on the relative changes in ozone induced by N_2O and CFC-11, neither of which degrade in the troposphere.

As shown in Figure 1a, total column ozone is sensitive to CO_2 and CH_4 and positively correlated with both. CO_2 and CH_4 lead to increased ozone abundances by cooling the stratosphere, which subsequently slows the gas-phase ozone loss cycles [*Jonsson et al.*, 2004]. Although CH_4 enhances the rate of the ozone-depleting HO_x chemistry in the upper stratosphere, its overall effect is to increase total column ozone via stratospheric cooling, production of tropospheric ozone, and by converting active chlorine to reservoir chlorine via reaction (R3) [*Fleming et al.*, 2011; *Revell et al.*, 2012c]:

$$CH_4 + Cl \rightarrow HCl + CH_3 \quad \text{(R3)}$$

The total column ozone changes shown in Figure 1a are in good agreement with previous sensitivity studies. For example, *Stolarski et al.* [2015] quantified ozone changes as a function of CO_2 and N_2O

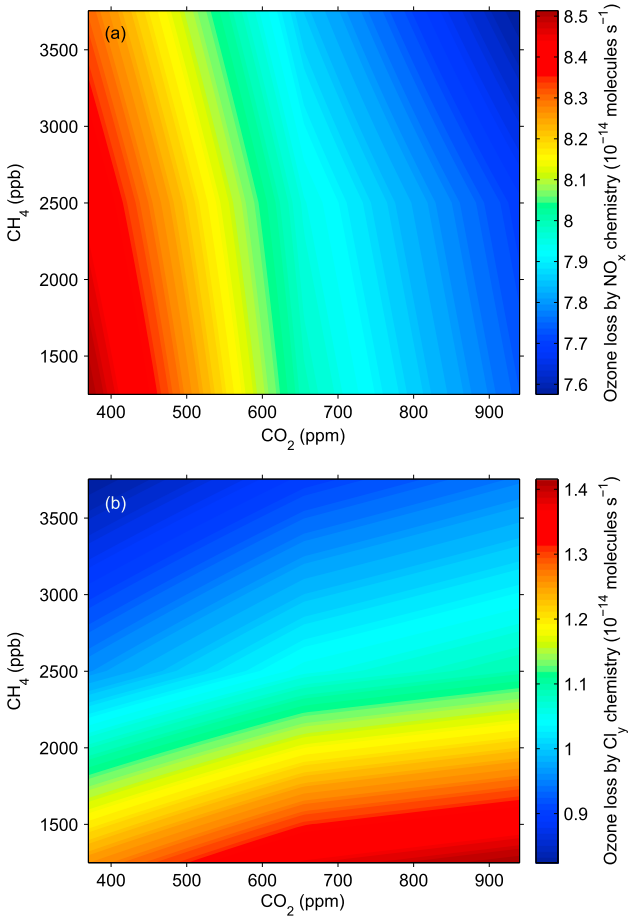

Figure 2. The sensitivity of ozone-depleting NO_x and Cl_y chemistry to CO_2 and CH_4 in the year 2100. (a) Global-annual-mean rate at which NO_x destroys ozone, integrated over the entire atmospheric column, for the nine sensitivity simulations. (b) As for Figure 2a but for the rate at which Cl_y destroys ozone.

concentrations. For the 2100 N_2O concentration corresponding to RCP 6.0 (406 ppb), and with constant CH_4 concentrations (1800 ppb), they showed that total column ozone increases by ~13 DU when the CO_2 concentration increases from 370 ppm to 940 ppm (the range of CO_2 concentrations in the present study). For the same N_2O and CH_4 concentrations, we find that total column ozone increases by ~12 DU for the equivalent CO_2 increase. *Revell et al.* [2012c] examined the sensitivity of ozone to CH_4 with constant CO_2 and N_2O concentrations and showed that for a 2505 ppb increase in CH_4 (the difference between the 2100 CH_4 concentration in RCP 2.6 and RCP 8.5), total column ozone increases by ~12 DU. For the same CO_2 concentration (but a larger N_2O concentration), we see an increase in total column ozone of ~15 DU.

3.2. ODPs for N_2O

We now assess the impact of N_2O on global-mean column ozone in year 2100 and how this is influenced by CO_2 and CH_4. We calculate the ODP of N_2O using equation (1). ODPs were developed as a straightforward policy instrument to evaluate the potential for long-lived halocarbons to deplete ozone relative to CFC-11 [*Harris and Wuebbles*, 2014]. We find $ODP_{N2O} = 0.015$ for the year 2000, which compares favorably with the value obtained by *Ravishankara et al.* [2009] of 0.017.

Traditionally, ODPs have been evaluated for the present-day atmosphere. However, given that N_2O is likely to remain the dominant ODS currently emitted by the end of the 21st century [*Ravishankara et al.*, 2009], we apply ODPs to a range of possible year 2100 atmospheres, as shown in Figure 1b. ODP_{N2O} ranges between 0.015 and 0.030, i.e., the same or twice as large as the year 2000 ODP, respectively. ODP_{N2O} in 2100 is larger than in 2000 for most of our sensitivity simulations, a finding consistent with *Ravishankara et al.* [2009], who showed that ODP_{N2O} may increase when stratospheric chlorine loading is smaller due to the buffering effect of chlorine on NO_x via (R2). We note that Figure 1b should not be literally interpreted to obtain values of ODP_{N2O}, given the discrepancies when the model is run with 39 or 90 vertical levels (discussed in section 3.3); rather it shows how ODP_{N2O} changes qualitatively in different CO_2 and CH_4 environments. Values of ODP_{N2O} are also displayed in Table S1 in the supporting information.

Given that increases in CO_2 and CH_4 lead to decreases in ozone-depleting NO_x chemistry (as discussed in section 1), one might hypothesize that the largest values of ODP_{N2O} would be obtained when ozone-depleting NO_x chemistry is fastest, i.e., in the simulation with the smallest CO_2 and CH_4 concentrations (Figure 2a). However, as shown in Figure 1b, ODP_{N2O} maximizes when CH_4 concentrations are largest. The explanation is that according to equation (1), a large value of ODP_{N2O} can be obtained not only by a mass unit of N_2O depleting more ozone but also by a mass unit of CFC-11 depleting less ozone.

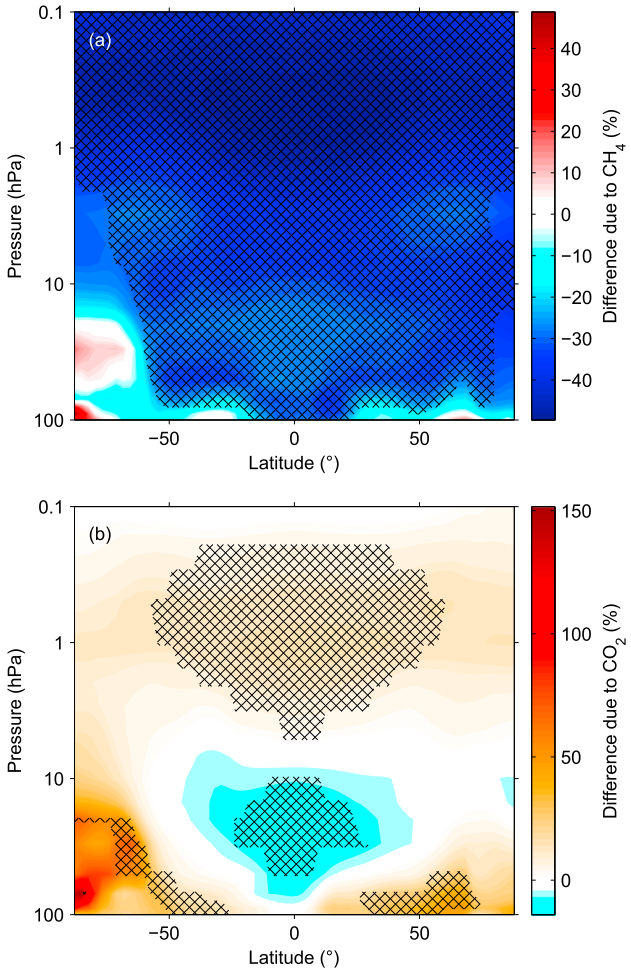

Figure 3. Difference in the annual-mean rate of the ozone-depleting Cl_y cycles in 2100, between (a) the high CH_4 and low CH_4 simulations with low CO_2 (high CH_4 minus low CH_4) and (b) the high CO_2 and low CO_2 simulations with low CH_4 (high CO_2 minus low CO_2). Hatching indicates that the differences are statistically significant at the 95% confidence level (calculated with the two-sample *t* test).

In the stratosphere, CFC-11 is photolyzed or undergoes reaction with $O(^1D)$ to produce Cl_y, which in turn participates in catalytic ozone loss cycles. Figure 2b shows that the effect of Cl_y on ozone is sensitive to CO_2 and CH_4, with the slowest Cl_y-induced ozone loss rates occurring when CH_4 concentrations are large and CO_2 concentrations are small. Large CH_4 concentrations slow the rate of Cl_y-induced ozone loss because CH_4 converts reactive chlorine via (R3) into HCl, which does not react directly with ozone, hence slowing Cl_y-induced ozone loss throughout the stratosphere (Figure 3a), except in the Antarctic lower stratosphere where CH_4 oxidation leads to additional H_2O, which in turn results in an enhancement of polar stratospheric clouds. Therefore, under high CH_4 and low CO_2 conditions ODP_{N2O} rises strongly because the ozone-depleting Cl_y cycles slow, rather than as a result of the effect of N_2O on ozone.

Rising levels of CO_2 can drive an increase as well as a decrease in Cl_y-induced ozone loss in various regions of the stratosphere, due to different processes. On one hand, a cooler stratosphere may lead to increased formation of polar stratospheric clouds, and therefore more heterogeneous chlorine chemistry and associated ozone loss in spring [*Austin et al.*, 1992]. Conversely, the Arctic polar vortex may become more unstable, for example, due to sudden stratospheric warmings, which may increase in frequency as the climate changes thus leading to less polar heterogeneous chlorine chemistry [*Langematz et al.*, 2014]. Furthermore, gas-phase chlorine chemistry is temperature-dependent and slows as CO_2 concentrations increase and the stratosphere cools [*Stolarski et al.*, 2015]. SOCOL shows that Cl_y chemistry slows in the extrapolar middle and lower stratosphere and becomes faster in the polar lower stratosphere, where the cooling effect on heterogeneous chemistry dominates (Figure 3b).

Recently, ODPs have been supplemented by the EESC (Equivalent Effective Stratospheric Chlorine) metric, which represents how much ozone will be destroyed as a function of the stratospheric evolution of chlorine and bromine, following surface release of various ODSs. *Daniel et al.* [2010] presented a method for including N_2O in the formulation of EESC, which requires ODP_{N2O} as an input term. As we have shown, the future sensitivity of the ozone layer to N_2O will be dependent on the time evolution of CO_2 and CH_4. Use of a single value for ODP_{N2O} found for the present-day atmosphere, in such an EESC-based formulation, might lead to unrealistic representation of the sensitivity of ozone to N_2O.

As well as CO_2 and CH_4, other atmospheric constituents may affect future ODP_{N2O}. As discussed in section 1, future increases in N_2O may impact ODP_{N2O}, because N_2O shortens its own lifetime [*Myhre and Shindell*, 2013]. Since we use the same surface N_2O concentrations for all of our sensitivity simulations, we do not

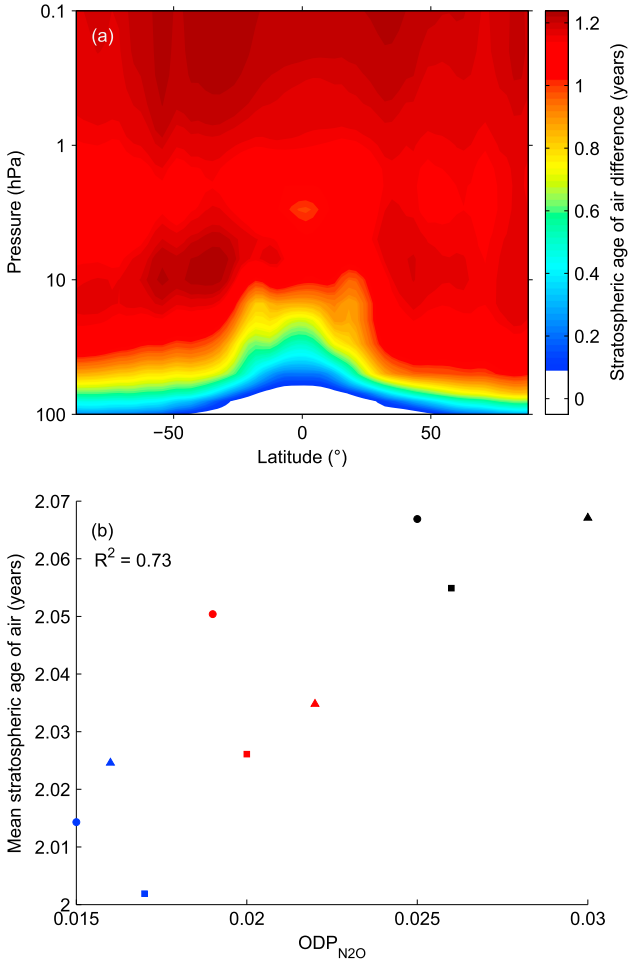

Figure 4. (a) Difference in the stratospheric age of air between identical SOCOL simulations performed with 39 and 90 vertical levels (90-level version minus 39-level version). (b) Mean stratospheric age of air versus ODP_{N2O}. Black markers: CO_2 = 370 ppm; red markers: CO_2 = 655 ppm; blue markers: CO_2 = 940 ppm. Circles: CH_4 = 1250 ppb; squares: CH_4 = 2502 ppb; triangles: CH_4 = 3755 ppb. Mean stratospheric age of air for the 90-level simulation = 2.87 years.

anticipate differences in our calculated values of ODP_{N2O} via this effect; however, experiments with different N_2O concentrations would conceivably yield different results. Furthermore, stratospheric aerosols are known to alter ODP_{N2O} [*Ravishankara et al.*, 2009]. When stratospheric aerosol loading is high, NO_x is converted to HNO_3 on aerosol surfaces, and therefore, ODP_{N2O} is lowered. Aerosols also affect ozone loss by Cl_y chemistry, which in turn affects ODP_{N2O} beyond changes in NO_x chemistry. Here we have considered only background aerosol from a volcanically quiescent period (year 2000) in our year 2100 simulations, as it is impossible to predict future volcanic eruptions. Should proposed stratospheric sulfate geoengineering schemes go ahead [*Crutzen*, 2006], projected year 2100 ODPs for N_2O would differ considerably from those presented here.

3.3. The Effect of Circulation Changes on ODP_{N2O}

A particular weakness of the SOCOL model is that the rate of tropical upwelling is too fast [*Stenke et al.*, 2013], which leads to shorter CFC-11 and N_2O lifetimes than calculated by other CCMs, and stratospheric air which is approximately 1 year younger than observations [*Chipperfield et al.*, 2014]. This age-of-air bias may systematically influence our ODP_{N2O} calculations, as with a slower rate of tropical upwelling there is more time for N_2O to undergo reaction with $O(^1D)$ to produce NO_x [*Plummer et al.*, 2010]. There is also more time for Cl_y to form from photochemical destruction of CFC-11; however, NO_x- and Cl_y-induced ozone loss occurs in different regions of the stratosphere.

Sensitivity experiments demonstrate that the age-of-air bias in SOCOL can be reduced (if not eliminated entirely) by running the model with 90-level vertical resolution, rather than the coarser 39-level version used in the present study. Figure 4a indicates that stratospheric air is approximately 1 year older in the 90-level version of the model. The disadvantage of the 90-level version of SOCOL is that it is computationally very expensive. To test the effect of the age-of-air bias on ODP_{N2O}, we ran one of the year 2100 sensitivity simulations (the low-CO_2 and low-CH_4 simulation) with the 90-level version of SOCOL and calculated an ODP_{N2O} of 0.040, compared with 0.025 in the 39-level version. Therefore, models without a circulation bias similar to that in the 39-level version of SOCOL should calculate larger values of ODP_{N2O}. The results presented in Figure 4b may assist in interpreting results from other models, as Figure 4b shows that ODP_{N2O} and the stratospheric mean age of air are positively correlated (R^2 = 0.73). However, due to nonlinear impacts of climate change, it is not clear that this relationship should necessarily be linear. With larger surface CO_2 mixing ratios, the Brewer-Dobson circulation strengthens (leading to a younger mean age of air), and there is less time available for N_2O to undergo reaction to produce NO_x. As a result, NO_x-induced ozone loss slows and ODP_{N2O} is smaller.

We anticipate that the values of ODP_{N2O} presented here are systematically smaller than would be obtained with other models, but that the demonstrated sensitivity of ODP_{N2O} to CO_2 and CH_4 is qualitatively correct.

4. Conclusions

The ODP concept is an integral part of national and international policymakers' considerations on ozone-protection policy, including the Montreal Protocol and its subsequent Adjustments and Amendments. ODPs arose as a means of determining the ability of a chemical to destroy ozone relative to CFC-11 and are normally found for the current atmosphere that has a well-defined composition. The advantage of using a ratio relative to another species is that for halocarbons, many uncertainties cancel. However, the interpretation for a nonhalocarbon GHG such as N_2O in future conditions is problematic, because the future atmospheric composition is so uncertain. Here we have demonstrated that differences of a factor of 2 occur for the future ODP_{N2O}, driven by the uncertainty in future levels of CH_4 and CO_2 that alter the future atmospheric chemical background, temperatures, and circulation.

As long as the Montreal Protocol continues to function effectively, N_2O will remain the dominant ODS emitted in the 21st century. Since N_2O and CFC-11 affect ozone differently in various CO_2 and CH_4 environments, a single ODP for N_2O is of limited use. Furthermore, given that GHG-induced changes in CFC-11-induced chemistry have such a large influence on ODP_{N2O}, the traditional approach of computing an ODP (i.e., computing the ratio of a perturbation of total column ozone induced by a specific compound relative to the change in ozone induced by a perturbation to CFC-11) further complicates quantitative assessment of the effect of N_2O on ozone. Model evaluation of the sensitivity of NO_x-induced ozone loss rates, as a function of future levels of CO_2 and CH_4 (i.e., Figure 2a) may provide a more meaningful method for assessing the effect of N_2O on ozone than the traditional approach.

Acknowledgments

L.E.R. acknowledges the SOCOL group at ETH Zurich and PMOD/WRC Davos for their ongoing efforts in developing the SOCOL model. L.E.R. was supported under the ETH Zurich Postdoctoral Fellowship Program. R.J.S. appreciates the support from NASA ACMAP. Data supporting the figures presented here are available by contacting the corresponding author.

References

Arfeuille, F., B. P. Luo, P. Heckendorn, D. Weisenstein, J. X. Sheng, E. Rozanov, M. Schraner, S. Brönnimann, L. W. Thomason, and T. Peter (2013), Modeling the stratospheric warming following the Mt. Pinatubo eruption: Uncertainties in aerosol extinctions, *Atmos. Chem. Phys.*, *13*, 11,221–11,234, doi:10.5194/acp-13-11221-2013.

Austin, J., N. Butchart, and K. P. Shine (1992), Possibility of an Arctic ozone hole in a doubled-CO_2 climate, *Nature*, *360*, 221–225, doi:10.1038/360221a0.

Chipperfield, M. P., et al. (2014), Multimodel estimates of atmospheric lifetimes of long-lived ozone-depleting substances: Present and future, *J. Geophys. Res. Atmos.*, *119*, 2555–2573, doi:10.1002/2013JD021097.

Crutzen, P. J. (1970), The influence of nitrogen oxides on the atmospheric ozone content, *Q. J. R. Meteorol. Soc.*, *96*, 320–325, doi:10.1002/qj.49709640815.

Crutzen, P. J. (2006), Albedo enhancement by stratospheric sulfur injections: A contribution to resolve a policy dilemma?, *Clim. Change*, *77*, 211–219, doi:10.1007/s10584-006-9101-y.

Daniel, J. S., E. L. Fleming, R. W. Portmann, G. J. M. Velders, C. H. Jackman, and A. R. Ravishankara (2010), Options to accelerate ozone recovery: Ozone and climate benefits, *Atmos. Chem. Phys.*, *10*, 7697–7707, doi:10.5194/acp-10-7697-2010.

ETH-PMOD (Swiss Federal Institute of Technology Zurich and the Physical-Meteorology Observatory Davos) Data (2015), Part of the Chemistry-Climate Model Initiative (CCMI-1) Project Database. NCAS British Atmospheric Data Centre. [Available at http://catalogue.ceda.ac.uk/uuid/1005d2c25d14483aa66a5f4a7f50fcf0.]

Eyring, V., et al. (2013), Long-term ozone changes and associated climate impacts in CMIP5 simulations, *J. Geophys. Res. Atmos.*, *118*, 5029–5060, doi:10.1002/jgrd.50316.

Fleming, E. L., C. H. Jackman, R. S. Stolarski, and A. R. Douglass (2011), A model study of the impact of source gas changes on the stratosphere for 1850–2100, *Atmos. Chem. Phys.*, *11*, 8515–8541, doi:10.5194/acp-11-8515-2011.

Harris, N. R. P., and D. J. Wuebbles (Lead Authors) (2014), Scenarios and information for policymakers, in *Scientific Assessment of Ozone Depletion: 2014*, *WMO Global Ozone Res. Monit. Proj. – Rep.*, vol. 55, Chap. 5, World Meteorol. Organization, Geneva, Switzerland.

Jonsson, A. I., J. de Grandpré, V. I. Fomichev, J. C. McConnell, and S. R. Beagley (2004), Doubled CO_2-induced cooling in the middle atmosphere: Photochemical analysis of the ozone radiative feedback, *J. Geophys. Res.*, *109*, D24103, doi:10.1029/2004JD005093.

Lamarque, J.-F., et al. (2010), Historical (1850–2000) gridded anthropogenic and biomass burning emissions of reactive gases and aerosols: Methodology and application, *Atmos. Chem. Phys.*, *10*, 7017–7039, doi:10.5194/acp-10-7017-2010.

Langematz, U., S. Meul, K. Grunow, E. Romanowsky, S. Oberländer, J. Abalichin, and A. Kubin (2014), Future Arctic temperature and ozone: The role of stratospheric composition changes, *J. Geophys. Res. Atmos.*, *119*, 2092–2112, doi:10.1002/2013JD021100.

Lin, S. J., and R. B. Rood (1996), Multidimensional flux-form semi-Lagrangian transport schemes, *Mon. Weather Rev.*, *124*(9), 2046–2070, doi:10.1175/1520-0493(1996)124<2046:MFFSLT>2.0.CO;2.

Luo, B. P. (2013), Stratospheric aerosol data for use in CCMI models, data files under. [Available at ftp://iacftp.ethz.ch/pub_read/luo/ccmi/, last accessed 9 August 2015.]

Masui, T., K. Matsumoto, Y. Hijioka, T. Kinoshita, T. Nozawa, S. Ishiwatari, E. Kato, P. R. Shukla, Y. Yamagata, and M. Kainuma (2011), An emission pathway for stabilization at 6 Wm-2 radiative forcing, *Clim. Change*, *109*(1–2), 59–76, doi:10.1007/s10584-011-0150-5.

Meehl, G. A., W. M. Washington, J. M. Arblaster, A. Hu, H. Teng, J. E. Kay, A. Gettelman, D. M. Lawrence, B. M. Sanderson, and W. G. Strand (2013), Climate change projections in CESM1(CAM5) compared to CCSM4, *J. Clim.*, *26*, 6287–6308, doi:10.1175/JCLI-D-12-00572.1.

Meinshausen, M., et al. (2011), The RCP greenhouse gas concentrations and their extensions from 1765 to 2300, *Clim. Change*, *109*, 213–241, doi:10.1007/s10584-011-0156-z.

Montzka, S. A., E. J. Dlugokencky, and J. H. Butler (2011), Non-CO_2 greenhouse gases and climate change, *Nature*, *476*, 43–50, doi:10.1038/nature10322.

Myhre, G., and D. Shindell (Coordinating Lead Authors) (2013), Anthropogenic and natural radiative forcing, in *Climate Change 2013: The Physical Science Basis. Contribution of Working Group I to the Fifth Assessment Report of the Intergovernmental Panel on Climate Change*, edited by T. F. Stocker et al., chap. 8, Cambridge Univ. Press, Cambridge, U. K., and New York.

Nakicenovic, N., and R. Swart (Eds.) (2000), *IPCC Special Report on Emissions Scenarios*, Cambridge Univ. Press, Cambridge, U. K.

Pawson, S., and W. Steinbrecht (Lead Authors) (2014), Update on global ozone: Past, present, and future, in *Scientific Assessment of Ozone Depletion: 2014*, *WMO Global Ozone Res. Monit. Proj. – Rep.*, vol. 55, Chap. 2, World Meteorol. Organization, Geneva, Switzerland.

Plummer, D. A., J. F. Scinocca, T. G. Shepherd, M. C. Reader, and A. I. Jonsson (2010), Quantifying the contributions to stratospheric ozone changes from ozone depleting substances and greenhouse gases, *Atmos. Chem. Phys.*, *10*, 8803–8820, doi:10.5194/acp-10-8803-2010.

Poeschl, U., R. von Kuhlmann, N. Poisson, and P. J. Crutzen (2000), Development and intercomparison of condensed isoprene oxidation mechanisms for global atmospheric modeling, *J. Atmos. Chem.*, *37*, 29–52, doi:10.1023/A:1006391009798.

Portmann, R. W., J. S. Daniel, and A. R. Ravishankara (2012), Stratospheric ozone depletion due to nitrous oxide: Influences of other gases, *Philos. Trans. R. Soc., B*, *367*, 1256–1264, doi:10.1098/rstb.2011.0377.

Prather, M. J. (1998), Time scales in atmospheric chemistry: Coupled perturbations to N_2O, NO_y, and O_3, *Science*, *279*, 1339–1341, doi:10.1126/science.279.5355.1339.

Ravishankara, A. R., J. S. Daniel, and R. W. Portmann (2009), Nitrous oxide (N_2O): The dominant ozone-depleting substance emitted in the 21st century, *Science*, *326*, 123–125, doi:10.1126/science.1176985.

Rayner, N. A., D. E. Parker, E. B. Horton, C. K. Folland, L. V. Alexander, D. P. Rowell, E. C. Kent, and A. Kaplan (2003), Global analyses of sea surface temperature, sea ice, and night marine air temperature since the late nineteenth century, *J. Geophys. Res.*, *108*(D14), 4407, doi:10.1029/2002JD002670.

Revell, L. E., G. E. Bodeker, D. Smale, R. Lehmann, P. E. Huck, B. E. Williamson, E. Rozanov, and H. Struthers (2012a), The effectiveness of N_2O in depleting stratospheric ozone, *Geophys. Res. Lett.*, *39*, L15806, doi:10.1029/2012GL052143.

Revell, L. E., G. E. Bodeker, P. E. Huck, and B. E. Williamson (2012b), Impacts of the production and consumption of biofuels on stratospheric ozone, *Geophys. Res. Lett.*, *39*, L10804, doi:10.1029/2012GL051546.

Revell, L. E., G. E. Bodeker, P. E. Huck, B. E. Williamson, and E. Rozanov (2012c), The sensitivity of stratospheric ozone changes through the 21st century to N_2O and CH_4, *Atmos. Chem. Phys.*, *12*, 11,309–11,317, doi:10.5194/acp-12-11309-2012.

Revell, L. E., F. Tummon, A. Stenke, T. Sukhodolov, A. Coulon, E. Rozanov, H. Garny, V. Grewe, and T. Peter (2015), Drivers of the tropospheric ozone budget throughout the 21st century under the medium-high climate scenario RCP 6.0, *Atmos. Chem. Phys.*, *15*, 5887–5902, doi:10.5194/acp-15-5887-2015.

Roeckner, E., et al. (2003), The atmospheric general circulation model ECHAM 5. Part I: Model description, Max-Planck-Institut für Meteorologie, Hamburg, Rep. 349. [Available at http://www.mpimet.mpg.de/fileadmin/publikationen/Reports/max_scirep_349.pdf.]

Rosenfield, J. E., and A. R. Douglass (1998), Doubled CO_2 effects on NO_y in a coupled 2D model, *Geophys. Res. Lett.*, *25*, 4381–4384, doi:10.1029/1998GL900147.

Solomon, S., M. Mills, L. E. Heidt, W. H. Pollock, and A. F. Tuck (1992), On the evaluation of ozone depletion potentials, *J. Geophys. Res.*, *97*, 825–842, doi:10.1029/91JD02613.

Stenke, A., M. Schraner, E. Rozanov, T. Egorova, B. Luo, and T. Peter (2013), The SOCOL version 3.0 chemistry-climate model: Description, evaluation, and implications from an advanced transport algorithm, *Geosci. Model Dev.*, *6*, 1407–1427, doi:10.5194/gmd-6-1407-2013.

Stolarski, R. S., A. R. Douglass, L. D. Oman, and D. W. Waugh (2015), Impact of future nitrous oxide and carbon dioxide emissions on the stratospheric ozone layer, *Environ. Res. Lett.*, *10*, 034011, doi:10.1088/1748-9326/10/3/034011.

WMO (2007), *Scientific Assessment of Ozone Depletion: 2006*, *WMO Global Ozone Res. Monit. Proj. – Rep.*, vol. 50, World Meteorol. Organization, Geneva, Switzerland.

WMO (2011), *Scientific Assessment of Ozone Depletion: 2010*, *WMO Global Ozone Res. Monit. Proj. – Rep.*, vol. 52, World Meteorol. Organization, Geneva, Switzerland.

Young, P. J., et al. (2013), Preindustrial to end 21st century projections of tropospheric ozone from the Atmospheric Chemistry and Climate Model Intercomparison Project (ACCMIP), *Atmos. Chem. Phys.*, *13*, 2063–2090, doi:10.5194/acp-13-2063-2013.